Hamilton-Jacobi Multi-Time Reachability

Manan Doshi[1,*], Manmeet Bhabra[1,*], Marius Wiggert[2], Claire J. Tomlin[2], and Pierre F.J. Lermusiaux[1]

***Abstract*— For the analysis of dynamical systems, it is fundamental to determine all states that can be reached at any given time. In this work, we obtain and apply new governing equations for reachability analysis over multiple start and terminal times all at once, and for systems operating in time-varying environments with dynamic obstacles and any other relevant dynamic fields. The theory and schemes are developed for both backward and forward reachable tubes with time-varying target and start sets. The resulting value functions elegantly capture not only the reachable tubes but also time-to-reach and time-to-leave maps as well as start time vs. duration plots and other useful secondary quantities for optimal control. We discuss the numerical schemes and computational efficiency. We first verify our results in an environment with a moving target and obstacle where reachability tubes can be analytically computed. We then consider the Dubin's car problem extended with a moving target and obstacle. Finally, we showcase our multi-time reachability in a non-hydrostatic bottom gravity current system. Results highlight the novel capabilities of exact multi-time reachability in dynamic environments.**

I. Introduction

Reachability analysis quantifies the states that can be reached by an actuated dynamical system. With optimal control, Hamilton-Jacobi (HJ) reachability analysis formalized this concept with differential equations, leading to recent successes [1], [2]. Classical HJ reachability is mainly concerned with the computation of reachable sets, forward and backward in time, often for robotics and autonomy applications. It provides analyses of the performance and safety of dynamical systems [1], including formal safety guarantees by determining regions of a system's state space that results in catastrophic failure (ex. hitting an obstacle) [3]. With some modifications, it handles moving obstacles and targets in both steady and time-varying systems [4], [5], [6], [7]. HJ reachability is a versatile method for path planning, even in complex environments such as strong and dynamic ocean currents [8], [9], [10]. It then provides the exact solution and is more efficient than other schemes, e.g., graph methods [11]. Reachability planning has been extended to uncertain environments [12] and risk optimality [13]. Finally, HJ reachability has been used in aircraft auto-landing, model predictive control (MPC) of unmanned aerial vehicles (UAVs) and underwater vehicles (AUVs), and multiplayer reach-avoid games [1], [14], [15], [16], [17], [18].

In this paper, the aim is to drastically extend reachability analysis. Some of the key questions that motivate our work include: i) How can we extend classical reachability theory to multiple start and terminal times?; ii) What is the corresponding value function that provides all level sets at once and what is its governing HJ reachability equation?; iii) Could we compute reachable tubes for all possible times without having to resort to repeated solves of classic reachability PDEs?; iv) What are other quantities that such multi-time forward and backward analysis could compute?; and v) What are the corresponding computational costs?

To address the above questions, we derive a new approach for analyzing the reachability of time-varying dynamical systems that we refer to as *multi-time reachability*. We formulate the optimal control problem using a new running cost term, and obtain new governing equations for reachability analysis over multiple start and terminal times all at once, and for systems operating in time-varying environments with dynamic obstacles and any other dynamic fields relevant to their control. Unlike the prior results on moving targets and obstacles, we present a theory that incorporates these effects in the system dynamics without introducing extra dimensions [4] and fields [7]. We apply our results to three applications and demonstrate that the new governing equations not only more efficiently compute backward and forward reachable tubes, but also generate new secondary quantities that encode valuable reachability information such as duration maps.

In what follows, Section II outlines the problem statement and introduce key notation. Section III develops the theory and equations for multi-time reachability. Numerical methods are briefly discussed in IV. In Section V, applications and numerical results for new multi-reachability problems are presented, followed by the conclusions in Section VI.

II. Problem Formulation

Our primary goal is to accurately and efficiently compute reachable tubes for general time-varying dynamical systems. There are essentially two main cases. In the first, we consider a time-varying target set and predict what is known as the backward reachable tube. In the second, we consider a time-varying start set and compute the forward reachable tube. For each case, we derive the governing equations and also solve the added complexity of time-varying obstacles that must be avoided in the dynamic environment.

Next, we formalize the above concepts. We define the properties of the dynamical systems. We then describe the start, target, and obstacle sets, as well as the backward

* M.D. and M.B. have contributed equally to this work.

[1] M.D., M.B., and P.F.J.L. are with the Department for Mechanical Engineering at MIT, USA. For inquiries contact: pierrel@mit.edu.

[2] M.W., and C.J.T. are with the Department of Electrical Engineering and Computer Sciences, University of California, Berkeley, USA.

We gratefully acknowledge the support of the C3.ai Digital Transformation Institute. P.F.J.L., M.D., and M.B. are grateful to the Office of Naval Research for partial support under Grant N00014-14-1-0476 (Science of Autonomy – LEARNS) to MIT as well as to the MIT Portugal Program for support under a MPP seed project and a Flagship program project (K2D).

and forward reachable tubes. Finally, we combine all these components and define the types of problems we solve.

A. System Dynamics

In this work, we consider dynamical systems defined by an ordinary differential equation (ODE) of the form

$$\dot{\boldsymbol{\xi}}(s) = \boldsymbol{f}(\boldsymbol{\xi}(s), \boldsymbol{u}(s), s), \quad s \in [0,T], \tag{1}$$

with given initial or terminal conditions, where $\boldsymbol{\xi} \in \mathbb{R}^{n_x}$ is the system state governed by the ODE, s the temporal variable in an interval $[0,T]$, and $\boldsymbol{u}(\cdot)$ the control from a set $\mathbb{U}$ of measurable functions of $s \in [0,T]$ with values in $\mathcal{U}$:

$$\mathbb{U} = \{\boldsymbol{\phi} : [0,T] \to \mathcal{U} \mid \boldsymbol{\phi}(\cdot) \text{ is measurable}\}. \tag{2}$$

The dynamical systems (1) govern state variables explicitly affected by the controls (e.g. autonomy variables) but the dynamics $\boldsymbol{f}$ in general includes all other relevant forcing such as the dynamic environment with dynamic obstacles and other dynamic fields that affect the autonomy, e.g. [19], [20]. The control space $\mathcal{U}$ is often a closed bounded set in $\mathbb{R}^{n_u}$, where n_u is the number of control inputs. The system dynamics $\boldsymbol{f} : \mathbb{R}^{n_x} \times \mathcal{U} \times \mathbb{R} \to \mathbb{R}^{n_x}$ are further assumed to be continuous, bounded and Lipschitz continuous in $\boldsymbol{\xi}$ uniformly in $\boldsymbol{u}$ [1]. Then, there exists a unique solution to Equation (1) for any control sequence $\boldsymbol{u}(\cdot)$ [21], [1]. For the initial value problem, this solution is the trajectory of the system from an initial state $\boldsymbol{x}$ at time $t \in [0,T]$ forced by the control sequence $\boldsymbol{u}(\cdot)$ and denoted here by $\boldsymbol{\xi}_{t,\boldsymbol{x}}^{\boldsymbol{u}(\cdot)}(s)$.

B. Start, Target, and Obstacle Sets

We focus on systems either launched from some dynamic start set or being required to reach a dynamic target set, with the constraint of avoiding the dynamic obstacle set, i.e. any dynamic disjoint obstacles that may be present. We now formalize some of the properties of these sets.

For each $t \in [0,T]$, we denote the time-varying start, target, and obstacle sets as $\mathcal{S}_t$, $\mathcal{T}_t$ and $\mathcal{O}_t$ respectively, where all sets are closed subsets of $\mathbb{R}^{n_x}$. Following closely [7], these sets, in turn, yield corresponding space-time sets $\mathbb{S}$, $\mathbb{O}$, and $\mathbb{T}$, which are all closed subsets of $\mathbb{R}^{n_x} \times [0,T]$:

$$\mathbb{S} \coloneqq \bigcup_{t\in[0,T]} \mathcal{S}_t \times \{t\}, \quad \mathbb{T} \coloneqq \bigcup_{t\in[0,T]} \mathcal{T}_t \times \{t\},$$
$$\mathbb{O} \coloneqq \bigcup_{t\in[0,T]} \mathcal{O}_t \times \{t\}. \tag{3}$$

The start, target, and obstacle sets are further assumed to evolve "smoothly" in time. Specifically, a set $\mathcal{M}_t$ is said to evolve smoothly in time if there exists a Lipschitz continuous function $\boldsymbol{g}_{\mathcal{M}}(\boldsymbol{\xi}) : \mathbb{R}^n \to \mathbb{R}^n$ such that for the system

$$\dot{\boldsymbol{\xi}} = \boldsymbol{g}_{\mathcal{M}}(\boldsymbol{\xi}), \tag{4}$$

all trajectories that start in $\mathcal{M}_t$ at some time t stay in the set $\mathcal{M}_{\bar{t}}$ at all subsequent times $\bar{t} \in [t,T]$. That is,

$$\boldsymbol{\xi}_{t,\boldsymbol{x}}(\bar{t}) \in \mathcal{M}_{\bar{t}} \quad \forall t \in [0,T],\ \forall \boldsymbol{x} \in \mathcal{M}_t,\ \forall \bar{t} \in [t,T]. \tag{5}$$

Practically, this implies that the dynamic start, target, and obstacle sets cannot teleport or disappear in the state space.

C. Reachability Sets and Tubes

In reachability analysis, backward and forward reachable sets or tubes are commonly needed [1]. The maximal sets and tubes encompass all the states to which the system can be driven to when going forward or backward through time, avoiding dynamic obstacles. These maximal sets and tubes can be defined as follows [3], [2], [1]:

1) Backward Reachable Set (BRS): Given a specified final time $t_f \in [0,T]$, the BRS at time $t \le t_f$ is the set of all states at time t that can reach a target set $\mathcal{T}_{t_f}$ *exactly* at the final time t_f:

$$\mathcal{R}(t,t_f,\mathcal{T}_{t_f},\mathbb{O}) = \{\hat{\boldsymbol{x}} \mid \exists \boldsymbol{u} \in \mathbb{U},\ \boldsymbol{x} = \hat{\boldsymbol{x}},$$
$$\boldsymbol{\xi}_{t,\boldsymbol{x}}^{\boldsymbol{u}(\cdot)}(t_f) \in \mathcal{T}_{t_f} \wedge \forall s \in [t,t_f],\ \boldsymbol{\xi}_{t,\boldsymbol{x}}^{\boldsymbol{u}(\cdot)}(s) \notin \mathcal{O}_s\}. \tag{6}$$

2) Backward Reachable Tube (BRT): BRTs extend BRSs. Given a specified final time $t_f \in [0,T]$, the BRT at time $t < t_f$ is the set of all states that can reach a time-varying target $\mathbb{T} \subset \mathbb{R}^{n_x} \times [0,T]$ at any time $\bar{t} \in [t,t_f]$:

$$\bar{\mathcal{R}}(t,t_f,\mathbb{T},\mathbb{O}) = \{\hat{\boldsymbol{x}} \mid \exists \boldsymbol{u} \in \mathbb{U},\ \exists \bar{t} \in [t,t_f],\ \boldsymbol{x} = \hat{\boldsymbol{x}},$$
$$\boldsymbol{\xi}_{t,\boldsymbol{x}}^{\boldsymbol{u}(\cdot)}(\bar{t}) \in \mathcal{T}_{\bar{t}} \wedge \forall s \in [t,t_f],\ \boldsymbol{\xi}_{t,\boldsymbol{x}}^{\boldsymbol{u}(\cdot)}(s) \notin \mathcal{O}_s\}. \tag{7}$$

3) Forward Reachable Set (FRS): Given a specified start time $t_s \in [0,T]$, the FRS at time $t \ge t_s$ is the set of all states that can be reached at time t when starting from a state within the set $\mathcal{S}_{t_s}$ at time t_s:

$$\mathcal{F}(t,t_s,\mathcal{S}_{t_s},\mathbb{O}) = \{\hat{\boldsymbol{x}} \mid \exists \boldsymbol{u} \in \mathbb{U},\ \exists \boldsymbol{x} \in \mathcal{S}_{t_s},$$
$$\boldsymbol{\xi}_{t_s,\boldsymbol{x}}^{\boldsymbol{u}(\cdot)}(t) = \hat{\boldsymbol{x}} \wedge \forall s \in [t_s,t],\ \boldsymbol{\xi}_{t_s,\boldsymbol{x}}^{\boldsymbol{u}(\cdot)}(s) \notin \mathcal{O}_s\} \tag{8}$$

4) Forward Reachable Tube (FRT): FRTs extend FRSs. Given a specified start time $t_s \in [0,T]$, the FRT at time $t > t_s$ is the set of all states that can be reached when launched from a state from a time-varying start set $\mathbb{S} \subset \mathbb{R}^{n_x} \times [0,T]$ at any time $\bar{t} \in [t_s,t]$:

$$\bar{\mathcal{F}}(t,t_s,\mathbb{S},\mathbb{O}) = \{\hat{\boldsymbol{x}} \mid \exists \boldsymbol{u} \in \mathbb{U},\ \exists \bar{t} \in [t_s,t],\ \exists \boldsymbol{x} \in \mathcal{S}_{\bar{t}},$$
$$\boldsymbol{\xi}_{\bar{t},\boldsymbol{x}}^{\boldsymbol{u}(\cdot)}(t) = \hat{\boldsymbol{x}} \wedge \forall s \in [\bar{t},t],\ \boldsymbol{\xi}_{\bar{t},\boldsymbol{x}}^{\boldsymbol{u}(\cdot)}(s) \notin \mathcal{O}_s\} \tag{9}$$

D. Problem Statement

Given a dynamical system of the form (1) operating in a dynamic environment with obstacles and possibly affected by other dynamic fields, our goal is to obtain equations that govern the backward and forward reachability tubes, as well as schemes that solve these equations efficiently:

1) Backward Reachability: Given a final time $t_f \in [0,T]$, a time $t < t_f$, and time-varying target and obstacle sets that define space-time sets $\mathbb{T}$ and $\mathbb{O}$, Eq. (3), we seek to derive and solve the equations for the BRTs, $\bar{\mathcal{R}}(t,t_f,\mathbb{T},\mathbb{O})$, Eq. (7).

2) Forward Reachability: Given a start time $t_s \in [0,T]$, a time $t > t_s$, and time-varying start and obstacle sets that define space-time sets $\mathbb{S}$ and $\mathbb{O}$, Eq. (3), we seek to derive and solve the equations for the FRTs, $\bar{\mathcal{F}}(t,t_s,\mathbb{S},\mathbb{O})$, Eq. (9).

Once the BRTs and/or FRTs are computed $\forall(t,t_f)$ and/or $\forall(t_s,t)$, they can be used to compute various other quantities of interest. Such quantities include: time-to-reach maps, i.e. maps of the minimum travel time to the target given the present state and time; start time vs. duration plots, i.e. function that maps the travel time to the target to the time at which the trajectory starts given a start state; and time-to-leave maps, i.e. maps of the latest time at which one can depart from the start state and reach the target point at a

given time. The computation of these secondary quantities is discussed in Section III-C.3

III. Multi-Time Reachability for Dynamic Sets

We now develop the theory and obtain the governing equations for HJ multi-time reachability for systems operating in dynamic environments. We start with multi-time reachability in the backward context, i.e. predict backward reachable tubes for time-varying target sets. We use continuous-time, optimal control and show how the resulting value function elegantly captures not only the backward reachable tubes but also time-to-reach maps. We then extend the results to the forward counterpart, i.e. predict forward reachable tubes for time-varying start sets. Finally, we present remarks and discuss secondary quantities such as time-to-reach and time-to-leave maps as well as start time vs. duration plots.

A. Backward Multi-Time Reachability

1) Augmented Dynamics: To account for the dynamic target and obstacle sets, we define a new augmented dynamical system as follows:

$$\dot{\boldsymbol{\xi}} = f_a(\boldsymbol{\xi}, \boldsymbol{u}, s) = \begin{cases} g_{\mathcal{O}}(\boldsymbol{\xi}, s), & \boldsymbol{\xi} \in \mathcal{O}_s \\ g_{\mathcal{T}}(\boldsymbol{\xi}, s), & \boldsymbol{\xi} \in \mathcal{T}_s \text{ and } \boldsymbol{\xi} \notin \mathcal{O}_s \\ f(\boldsymbol{\xi}, \boldsymbol{u}, s), & \text{otherwise} \end{cases}. \tag{10}$$

where $g_{\mathcal{O}}(\boldsymbol{\xi}, s)$ and $g_{\mathcal{T}}(\boldsymbol{\xi}, s)$ are functions that keep trajectories within their respective sets as defined by Eq. (4). With this augmentation, we provide valuable properties to the system. First, once a state enters an obstacle set, it will remain in that set for all subsequent times irrespective of the controls applied. Second, the same holds for states that enter the target set. These properties will be shown to be key in our optimal control setting.

2) Optimal Control: For our optimal control problem, we first define the terminal cost at time T,

$$l_{term}(\boldsymbol{\xi}) = \begin{cases} \infty, & \boldsymbol{\xi} \in \mathcal{O}_T \\ d(\boldsymbol{\xi}, \mathcal{T}_T), & \text{otherwise} \end{cases}. \tag{11}$$

Eq. (11) defines the terminal cost of a state in the obstacle set to be infinitely high (in Section IV we address how this property can be numerically handled). For all other states, the cost is defined as the distance of the state ($\boldsymbol{\xi}$) from the target set at the terminal time ($\mathcal{T}_T$) under some distance metric d which depends on the system at hand. Being a distance metric, we require $d(\boldsymbol{\xi}, \mathcal{T}_T) \geq 0 \; \forall (\boldsymbol{\xi}, \mathcal{T}_T)$ and $d(\boldsymbol{\xi}, \mathcal{T}_T) = 0$ if and only if $\boldsymbol{\xi} \in \mathcal{T}_T$.

The running cost is defined as a constant negative value at the target set and zero everywhere else

$$l(\boldsymbol{\xi}, s) = \begin{cases} -\alpha, & \boldsymbol{\xi} \in \mathcal{T}_s \text{ and } \boldsymbol{\xi} \notin \mathcal{O}_s \\ 0, & \text{otherwise} \end{cases}, \tag{12}$$

where α is an arbitrary positive constant which we set to 1. The solution is exact irrespective of the value of α. Values of α can however be used to minimize numerical errors due to discontinuities that arise out of this loss function (not shown).

Using the augmented dynamics (10), terminal cost (11), and running cost (12), the total cost function incurred when using controls $\boldsymbol{u}(\cdot)$ and initial state $\boldsymbol{x}$ at initial time t is

$$J(\boldsymbol{x}, \boldsymbol{u}(\cdot), t) = l_{term}(\boldsymbol{\xi}_{t,\boldsymbol{x}}^{\boldsymbol{u}(\cdot)}(T)) + \int_t^T l(\boldsymbol{\xi}_{t,\boldsymbol{x}}^{\boldsymbol{u}(\cdot)}(s), s) ds \tag{13}$$

To obtain an intuition for the meaning of the total cost, we substitute the functions for the case when the trajectory $\boldsymbol{\xi}_{t,\boldsymbol{x}}^{\boldsymbol{u}(\cdot)}(s)$ never enters the obstacle set,

$$J(\boldsymbol{x}, \boldsymbol{u}(\cdot), t) = \underbrace{d(\boldsymbol{\xi}_{t,\boldsymbol{x}}^{\boldsymbol{u}(\cdot)}(T), \mathcal{T}_T)}_{\substack{\text{Terminal distance} \\ \text{from target set}}} - \alpha \underbrace{\int_t^T \mathbb{I}_{\mathcal{T}_s}\left(\boldsymbol{\xi}_{t,\boldsymbol{x}}^{\boldsymbol{u}(\cdot)}(s)\right) ds}_{\substack{\text{Time spent} \\ \text{in target set}}} \tag{14}$$

where the identity function $\mathbb{I}_{\mathcal{T}_s}(\boldsymbol{\xi}) = 1$ when $\boldsymbol{\xi} \in \mathcal{T}_s$ and is 0 otherwise. We note that if the trajectory ever enters the obstacle set, it will stay in the obstacle set at the terminal time under the augmented dynamics and will incur an infinitely high total cost. Additionally, the value function under the optimal control for trajectories that avoids the obstacles is,

$$J^*(\boldsymbol{x}, t) = \min_{\boldsymbol{u}(\cdot) \in \mathbb{U}} \left[d(\boldsymbol{\xi}_{t,\boldsymbol{x}}^{\boldsymbol{u}(\cdot)}(T), \mathcal{T}_T) - \alpha \int_t^T \mathbb{I}_{\mathcal{T}_s}\left(\boldsymbol{\xi}_{t,\boldsymbol{x}}^{\boldsymbol{u}(\cdot)}(s)\right) ds \right] \tag{15}$$

To explain this minimization physically, we consider two cases. In the first, we assume there exists some control that drives the system from initial state $\boldsymbol{x}$ (or set) at time t into the target set at a time $\bar{t} \in [t, T]$ while avoiding the obstacles. In the opposive second, we assume no control can drive the system to the target set while avoiding the obstacles.

a) Case 1: Let $\boldsymbol{u}^*(\cdot)$ be the set of controls that drives the system from state $\boldsymbol{x}$ at time t (under the augmented dynamics) to the target set at the earliest possible time $t^* = \min(\bar{t})$ while avoiding the dynamic obstacle set $\mathbb{O}$. We reiterate that for the augmented system (10), if the target set is reached at some $t^* < T$, the system will stay in the set at all future times and hence $\boldsymbol{\xi}_{t,\boldsymbol{x}}^{\boldsymbol{u}(\cdot)}(T) \in \mathcal{T}_T$. It follows then that the cost for such a set of controls is:

$$\begin{aligned} J(\boldsymbol{x}, \boldsymbol{u}^*(\cdot), t) &= \underbrace{d(\boldsymbol{\xi}_{t,\boldsymbol{x}}^{\boldsymbol{u}(\cdot)}(T), \mathcal{T}_T)}_{0} - \alpha \underbrace{\int_t^T \mathbb{I}_{\mathcal{T}_s}\left(\boldsymbol{\xi}_{t,\boldsymbol{x}}^{\boldsymbol{u}(\cdot)}(s)\right) ds}_{T - t^*} \\ &= -\alpha(T - t^*). \end{aligned}$$

We now provide the lower bound of the value function (15) under the optimal control

$$\begin{aligned} J^*(\boldsymbol{x}, t) &= \min_{\boldsymbol{u}(\cdot) \in \mathbb{U}} \Big[d(\boldsymbol{\xi}_{t,\boldsymbol{x}}^{\boldsymbol{u}(\cdot)}(T), \mathcal{T}_T) - \\ &\qquad \alpha \int_t^T \mathbb{I}\left\{\boldsymbol{\xi}_{t,\boldsymbol{x}}^{\boldsymbol{u}(\cdot)}(s) \in \mathcal{T}_s\right\} ds \Big] \qquad (16) \\ &\geq \min_{\boldsymbol{u}(\cdot) \in \mathbb{U}} \left[d(\boldsymbol{\xi}_{t,\boldsymbol{x}}^{\boldsymbol{u}(\cdot)}(T), \mathcal{T}_T) \right] \\ &\qquad + \min_{\boldsymbol{u}(\cdot) \in \mathbb{U}} \left[-\alpha \int_t^T \mathbb{I}\left\{\boldsymbol{\xi}_{t,\boldsymbol{x}}^{\boldsymbol{u}(\cdot)}(s) \in \mathcal{T}_s\right\} ds \right] \qquad (17) \\ J^*(\boldsymbol{x}, t) &\geq -\alpha(T - t^*). \qquad (18) \end{aligned}$$

This lower bound is achieved under the control $\boldsymbol{u}^*$. Therefore, when the vehicle can reach the destination, the optimal control under the given loss function generates a time optimal trajectory to the target state. The value function is given by $J^*(\boldsymbol{x}, t) = -\alpha(T - t^*)$ where t^* is the minimum time at which a trajectory starting at $(\boldsymbol{\xi}, t)$ can reach the target state.

b) Case 2: When there exists no control $\boldsymbol{u}(\cdot)$ that can drive the system from $(\boldsymbol{x}, t)$ to the target set while avoiding the obstacles, the term $\mathbb{I}_{\mathcal{T}_s}\left(\boldsymbol{\xi}_{t,\boldsymbol{x}}^{\boldsymbol{u}(\cdot)}(s)\right)$ in the value function (15) is always 0 by construction. It follows then that:

$$J^*(\boldsymbol{x}, t) = \min_{\boldsymbol{u}(\cdot)\in\mathbb{U}} \left[l_{term}(\boldsymbol{\xi}_{t,\boldsymbol{x}}^{\boldsymbol{u}(\cdot)}(T))\right] \tag{19}$$

That is, when a trajectory with initial conditions $(\boldsymbol{x}, t)$ cannot reach the target set, the minimization of the cost function will lead the system as close to the target set as possible while avoiding the obstacle (since hitting the obstacle will drive the terminal cost infinitely high).

To summarize, the value function corresponding to the optimal control problem is given as

$$J^*(\boldsymbol{x}, t) = \begin{cases} -\alpha(T - \min(\bar{t})), & \text{if } \exists \boldsymbol{u}(\cdot) \text{ s.t.} \\ & \boldsymbol{\xi}_{t,\boldsymbol{x}}^{\boldsymbol{u}(\cdot)}(\bar{t}) \in \mathcal{T}_{\bar{t}} \\ \infty, & \text{if } \nexists \boldsymbol{u}(\cdot) \text{ s.t.} \\ & \boldsymbol{\xi}_{t,\boldsymbol{x}}^{\boldsymbol{u}(\cdot)}(\bar{t}) \notin \mathcal{O}_{\bar{t}} \\ & \forall \bar{t} \in [t, T] \\ \min_{\boldsymbol{u}} d(\boldsymbol{\xi}_{t,\boldsymbol{x}}^{\boldsymbol{u}(\cdot)}(T), \mathcal{T}_T), & \text{Otherwise.} \end{cases} \tag{20}$$

In other words, at any state $\boldsymbol{x}$ at a time $t \in [0, T]$, the value of $J^*(\boldsymbol{x}, t)$, if negative, physically implies that a state starting at $\boldsymbol{x}$ at time t can reach the target set before the terminal time T. Moreover, the earliest time that it can reach the destination is given by $T + \frac{J^*(\boldsymbol{x},t)}{\alpha}$. If the value of $J^*(\boldsymbol{x}, t)$ is positive, it implies that a state starting at $\boldsymbol{x}$ at time t cannot reach the target set in the time interval $[t, T]$, and the value physically corresponds to how close such a state could possibly get to the target set at the terminal time T. Finally, for states for which $J^*(\boldsymbol{x}, t)$ is infinite, we have that for a system starting at $\boldsymbol{x}$ at time t, the obstacle will inevitably be hit.

3) The Hamilton-Jacobi-Bellman Equation: The value function can be efficiently computed using dynamic programming. For continuous-time optimal control, it is the viscosity solution of the Hamilton-Jacobi-Bellman (HJB) partial differential equation (PDE) [22], [23], [24]

$$\frac{\partial J^*(\boldsymbol{x}, t)}{\partial t} + \min_{\boldsymbol{u}} \left[l(\boldsymbol{x}, t) + \nabla_{\boldsymbol{x}} J^* \cdot f_a(\boldsymbol{x}, \boldsymbol{u}, t)\right] = 0$$
$$J^*(\boldsymbol{x}, T) = l_{term}(\boldsymbol{x}), \tag{21}$$

where l_{term} and l are the terminal and running costs, respectively. For our problem, these costs are defined in Eqs. (11) and (12). Inserting them and the augmented dynamical system (10) in Eq. (21), we obtain the final HJB PDE:

$$\frac{\partial J^*(\boldsymbol{x}, t)}{\partial t} = \begin{cases} -\left[-\alpha + \nabla_{\boldsymbol{x}} J^* \cdot g_{\mathcal{T}}(\boldsymbol{x}, t)\right], & \boldsymbol{x}(t) \in \mathcal{T}_t \cap (\mathcal{O}_t)^c \\ -\left[\nabla_{\boldsymbol{x}} J^* \cdot g_{\mathcal{O}}(\boldsymbol{x}, t)\right], & \boldsymbol{x}(t) \in \mathcal{O}_t \\ -\min_{\boldsymbol{u}} \left[\nabla_{\boldsymbol{x}} J^* \cdot f(\boldsymbol{x}, \boldsymbol{u}, t)\right], & \text{otherwise} \end{cases}$$

$$J^*(\boldsymbol{x}, T) = \begin{cases} \infty, & \boldsymbol{x} \in \mathcal{O}_T \\ d(\boldsymbol{x}, \mathcal{T}_T), & \text{otherwise} \end{cases}. \tag{22}$$

Eq. (22) is a terminal-value problem which is solved backward in time to obtain the value of $J^*(\boldsymbol{x}, t)$ for all states in the state space and all times $t \in [0, T]$.

4) Equation for Backward Reachable Tubes: Using the value function J^* governed by the HJB PDE (22), we now obtain the equation for the BRTs defined by Eq. (7) as well as an efficient scheme for their computation. Consider a fixed time $t_f \in [0, T]$ and a time $t < t_f$. From Eq. (20), it follows that for any state $\boldsymbol{x}$ satisfying $J^*(\boldsymbol{x}, t) \leq -\alpha(T - t_f)$, a control function $\boldsymbol{u}(\cdot)$ exists that will drive the system from state $\boldsymbol{x}$ at time t to the target set at some time $\bar{t} \in [t, t_f]$. This results in an efficient scheme to compute the BRT:

$$\bar{\mathcal{R}}(t, t_f, \mathbb{T}, \mathbb{O}) = \{\boldsymbol{x} \mid J^*(\boldsymbol{x}, t) \leq -\alpha(T - t_f)\}. \tag{23}$$

For a specified final time t_f, the BRT at any time $t < t_f$ can simply be extracted by considering the appropriate sub-level set of the value function at that time. This is because an agent in this set would reach the target while avoiding the obstacle at $t < t_f$ under the optimal control and stay in the target because of the augmented dynamics 10 accumulating the negative cost at the destination.

5) Equation for Time-to-Reach Maps: The value function stores important information regarding the optimal time a system can reach the target set. This can be used to compute time-to-reach or duration maps $\mathcal{D}$ from Eq. (21) or (22):

$$\mathcal{D}(\boldsymbol{x}, t) = T + \frac{J^*(\boldsymbol{x}, t)}{\alpha} - t, \qquad \forall (\boldsymbol{x}, t) \text{ s.t. } J^*(\boldsymbol{x}, t) < 0.$$

For a state $\boldsymbol{x}$ at time t satisfying $J^*(\boldsymbol{x}, t) \leq 0$, Eq. (20) implies that such a state can reach the target set and the earliest possible time this will happen will be at $T + \frac{J^*(\boldsymbol{x},t)}{\alpha}$. It follows then that for all $(\boldsymbol{x}, t)$ with $J^*(\boldsymbol{x}, t) \leq 0$, $\mathcal{D}(\boldsymbol{x}, t)$ corresponds to the minimum duration for a trajectory starting at state $\boldsymbol{x}$ at time t to reach the target set.

6) Closed-loop optimal controller: As discussed in Section III-A.2, an optimal controller that minimizes the cost function will: (a) avoid dynamic obstacles; (b) reach the target in minimum time if it can; and (c), reach as close to the target as possible if it cannot reach it. The optimal controller can also compute the minimum duration to the target set from the current state. Thus, solving for $J^*(\boldsymbol{x}, t)$ using Eq. (22) provides a powerful closed-loop control policy:

$$\pi(\boldsymbol{x}, t) = \arg\min_{\boldsymbol{u}} \left[\nabla_{\boldsymbol{x}} J^*(\boldsymbol{x}, t) \cdot f(\boldsymbol{x}, \boldsymbol{u}, t)\right] \ \forall \boldsymbol{x} \notin (\mathcal{O}_t \cup \mathcal{T}_t) \ ,$$

as demonstrated with reliable navigation in complex time-varying ocean currents with forecast errors [25].

B. Forward Multi-Time Reachability

Section III-A addressed backward multi-time reachability. That is, we considered how to efficiently compute backward reachable tubes (and time-to-reach maps) in a dynamic environment with time-varying target and obstacle sets. In this section, we examine the forward counterpart, and derive how to compute forward reachable tubes in dynamic domains containing now time-varying start sets.

The forward problem can be addressed analogously to the derivation in Section III-A, but now analyzing the system evolution *backwards* in time. First, an augmented dynamic system akin to Eq. (10) can be defined as follows:

$$\dot{\boldsymbol{\xi}} = \tilde{f}_a(\boldsymbol{\xi}, \boldsymbol{u}, s) = \begin{cases} g_{\mathcal{O}}(\boldsymbol{\xi}, s), & \boldsymbol{\xi} \in \mathcal{O}_s \\ g_{\mathcal{S}}(\boldsymbol{\xi}, s), & \boldsymbol{\xi} \in \mathcal{S}_s \text{ and } \boldsymbol{\xi} \notin \mathcal{O}_s \\ f(\boldsymbol{\xi}, \boldsymbol{u}, s), & \text{otherwise} \end{cases}. \tag{24}$$

where now the start set is used instead of the target set. This system's evolution backwards in time can be studied by mapping time to a new "reverse-time" variable, $\tau(t) = T - t$, resulting in a mapped augmented dynamical system:

$$\frac{d\boldsymbol{\xi}}{d\tau} = -\tilde{f}_a(\boldsymbol{\xi}, \boldsymbol{u}, T - \tau) \, . \tag{25}$$

Analogous to backward multi-time reachability, we can formulate an optimal control for the system (25) while using the start set in place of the target set. Specifically, we define a terminal cost, now at time $\tau = T$, of the form:

$$\tilde{l}_{term}(\boldsymbol{\xi}) = \begin{cases} \infty, & \boldsymbol{\xi} \in \mathcal{O}_0 \\ d(\boldsymbol{\xi}, \mathcal{S}_0), & \text{otherwise} \end{cases}. \tag{26}$$

To remain consistent with the set indexing convention introduced in Section II-B, the sets in Eq. (26) are evaluated at time $t = 0$ (corresponds to the "terminal" reverse-time $\tau = T$). Moreover, a running cost can be similarly defined:

$$\tilde{l}(\boldsymbol{\xi}, \tau) = \begin{cases} -\alpha, & \boldsymbol{\xi} \in \mathcal{S}_{(T-\tau)} \text{ and } \boldsymbol{\xi} \notin \mathcal{O}_{(T-\tau)} \\ 0, & \text{otherwise} \end{cases}, \tag{27}$$

The value function for this optimal control problem can again be computed by forming a HJB PDE using now the dynamical system (24), terminal cost (26), and running cost (27). Mapping the resulting HJB PDE back to the original time variable t so as to not have to explicitly work in reverse-time τ, the HJB PDE can be shown to be given as:

$$\frac{\partial \tilde{J}^*(\boldsymbol{x}, t)}{\partial t} + \max_{\boldsymbol{u}} \left[-\tilde{l}(\boldsymbol{x}, t) + \nabla_{\boldsymbol{x}} \tilde{J}^* \cdot \tilde{f}_a(\boldsymbol{x}, \boldsymbol{u}, t) \right] = 0$$
$$\tilde{J}^*(\boldsymbol{x}, 0) = \tilde{l}_{term}(\boldsymbol{x}), \tag{28}$$

which, upon inserting the augmented dynamics (24), and the costs (26) and (27), yields:

$$\frac{\partial \tilde{J}^*(\boldsymbol{x}, t)}{\partial t} = \begin{cases} -\left[\alpha + \nabla_{\boldsymbol{x}} J^* \cdot g_{\mathcal{S}}(\boldsymbol{x}, t)\right], & \boldsymbol{x}(t) \in \mathcal{S}_t \cap (\mathcal{O}_t)^c \\ -\left[\nabla_{\boldsymbol{x}} J^* \cdot g_{\mathcal{O}}(\boldsymbol{x}, t)\right], & \boldsymbol{x}(t) \in \mathcal{O}_t \\ -\max_{\boldsymbol{u}} \left[\nabla_{\boldsymbol{x}} J^* \cdot f(\boldsymbol{x}, \boldsymbol{u}, t)\right], & \text{Otherwise} \end{cases}$$

$$\tilde{J}^*(\boldsymbol{x}, 0) = \begin{cases} \infty, & \boldsymbol{x} \in \mathcal{O}_0 \\ d(\boldsymbol{x}, \mathcal{S}_0), & \text{otherwise} \end{cases}. \tag{29}$$

In duality to the backward multi-reach setting where a terminal-value problem was obtained, in this case the value function $\tilde{J}^*(\boldsymbol{x}, t)$ is given as the solution to an initial value problem. Furthermore, analogous to the backward setting, the value function can be used to extract the FRT,

$$\bar{\mathcal{F}}(t, t_s, \mathbb{S}, \mathbb{O}) = \{\boldsymbol{x} \mid \tilde{J}^*(\boldsymbol{x}, t) \leq -\alpha \cdot t_s\}, \tag{30}$$

and the time-to-leave maps,

$$\tilde{\mathcal{D}}(\boldsymbol{x}, t) = -\frac{\tilde{J}^*(\boldsymbol{x}, t)}{\alpha}, \qquad \forall (\boldsymbol{x}, t) \text{ s.t., } \tilde{J}^*(\boldsymbol{x}, t) < 0. \tag{31}$$

In comparison to backward reachability, the optimal controller obtained by working in reverse-time allows computing the start set as quickly as possible in a reverse-time setting. This is not as commonly useful since the universe runs forward in time, thus usually requiring an open-loop controller to execute the corresponding trajectories.

C. Remarks and Discussion

With the evolution equations derived for multi-time reachability, we now present several properties and differences when compared to classic reachability.

1) Ability to compute BRTs/FRTs with arbitrary start and end times: We note that we require a single solve of the PDE 22/29 to compute all possible BRTs/FRTs for a given dynamical system, target/start set, and obstacle set using Eq. (23)/(30). With classic reachability, one would instead a solve of a HJB PDE for every terminal time t_f, or start time t_s. While this benefit is inconsequential when dealing with a time-invariant system (since the backward and forward reachability tubes depend only on the time duration, $t_f - t$ and $t - t_s$, respectively), this property is very useful for analyzing dynamic systems. Many multi-time autonomy problems today indeed involve dynamic environments governed by PDEs (e.g., UAVs or AUVs affected by currents or winds), dynamic target/start sets, and/or dynamic obstacle sets [26]. Multi-time reachability thus has strong appeal.

While finishing this work, [27] posted a related framework that also adds a running cost to the HJB equation. Presently however, we derive and apply the exact governing equations for BRTs/FRTs and associated quantities, for the first time for systems operating in time-varying environments with dynamic obstacles and affected by other dynamic fields.

2) Field of Level Sets: In classical reachability, only the data on the zero level set of the value function is typically used, as this decomposes the space into the reachable and non-reachable regions which is usually what is of interest In multi-time reachability, a PDE of essentially identical complexity is solved, yet every value on the field provides useful physical reachability information. Specifically, in the backward reachability setting, the physical meaning of other level sets of the value function is given by Eq. (20). In this case, we reiterate, level sets with a negative value provide minimum times at which a target set can be reached from a given state, level sets with a positive value correspond to the closest distance to the target that can be reached for states that cannot reach the target, and finally an infinite value for J^* are states where it is unavoidable that an obstacle will be hit. The case of forward reachability has a similar physical interpretation for its different level sets.

3) Secondary quantities: While the value function obtained by classical backward reachability determines if one can reach the destination by time t_f given a starting time and position, the value function obtained using multi-time backward reachability determines *when* one can reach the target set ($\mathcal{D}(\boldsymbol{x}, t)$). When evaluated at a given position $\boldsymbol{x}$, one can infer the map between the starting time of the trajectory to the duration it takes to reach the target. Similarly, the forward value function determines *when* to start a journey to be able to reach an arbitrary point from the starting set ($\tilde{\mathcal{D}}(\boldsymbol{x}, t)$). This information can be extremely valuable for time varying systems where the time to reach the destination can vary drastically with the time at which the trajectory starts. We refer to the resulting plots as duration vs. arrival time, and start time vs. duration.

4) Optimal Controller: The closed loop controller under the value function for multi-time reachability (Sect. III-A.6) has varied desirable properties including obstacle avoidance, time optimality if the target is reachable, and distance to target minimized if not. This drastically augments classical reachability that only minimizes the terminal signed distance from the target set at time T and does not provide time optimality when the state is not on the zero level set.

IV. Computation and Numerical Schemes

In Section III, the PDEs (21)-(22) for the value function of backward reachability and PDEs (28)-(29) for the value function of forward reachability are HJB PDEs. These PDEs, including the existence, uniqueness, and properties of their viscosity solutions, have been extensively studied in recent years due to their broad applicability [28], [29], [22].

Several options exist for numerically computing a viscosity solution to a given HJB PDE, ranging from Finite Volume methods to high-order discontinuous Galerkin methods [30], [31], [32], [9], [26]. Presently, we used the method of lines, with high-order finite difference methods for the temporal and spatial discretization, on structured, uniform, rectangular meshes [33], [34]. Our software was built on top of an open-source HJ equation solver, hj_reachability [35], built on JAX [36]. To numerically compute the viscosity solution, the Local Lax-Friedrichs scheme was used [29], [33], [34].

Since the above scheme is fully explicit, the computational cost is $\mathcal{O}(N_x N_t)$ where N_x and N_t are the total number of spatial gridpoints and of timesteps, respectively. The explicit scheme allows direct parallelization of the computation across gridpoints. The cost of our method is thus exactly of the same order as that of classical reachability while providing much richer information about the system.

Finally, we discuss two numerical implementation details: (1) Handling the infinite condition in the terminal cost for when a state terminates in an obstacle set, i.e. Eqs. (11) and (26), is straightforward. Since the numerical solve is inherently restricted to a closed and bounded state space, we simply set the terminal cost value when in an obstacle set to an arbitrary constant greater than the largest possible signed distance value in the domain at terminal time. When processing the final numerically computed value function, we simply mask off all values that equal this arbitrary constant as there are no controls that allow the system to avoid the obstacle. (2) The constant α in Eq. (12) can be chosen to decrease round off errors associated to the numerical solve. By setting α to the order of the characteristic time of the problem, the contours of interest will be $\mathcal{O}(1)$.

V. Numerical Results

We illustrate our theory and schemes on three numerical cases. In the first, we verify our method by applying it to a system with analytical reachability tubes. In the second and third cases, we consider more complex systems and demonstrate the various capabilities of our approach.

A. Analytical Moving Target and Obstacle

1) Problem Setup: This case uses the example of [7, Sec 5.1]. The 2D dynamical system consists of a vehicle moving with a constant speed in any heading, $\dot{\boldsymbol{x}} = u_{veh}\hat{\boldsymbol{h}}$, where the state $\boldsymbol{x} = [x, y]$ is the vehicle position, $\hat{\boldsymbol{h}}$ the unit heading, and $u_{veh} = 0.5$ the constant speed of the vehicle. The dynamic target set is a square of side length 0.4 units centered at $[0, 0.75]$ at $t = 0$ travelling with velocity of $[0, -1.5]$ units. The obstacle is a square of side length 0.2 initially centered at $[0, 0]$ and traveling with velocity of $[0, -1]$ units. Our goal is to compute backward reachability tubes and compare them to the analytical solution we obtained geometrically using [7, Sec 5.1.1]. The augmented dynamics is here straightforward: we modify the system dynamics such that when the agent is in the target (/obstacle) it moves exactly with the known velocity of the target (/obstacle).

2) Results: Fig. 1 shows the analytical, overlaid on the numerical, backward reachability tubes using our multi-time reachability. The analytical and numerical tubes (left half of the domain) are effectively identical. When compared to the results in [7] that compute the BRTs for $t_f = 0.5$, our approach accurately computes tubes for all terminal times t_f and in a single PDE simulation.

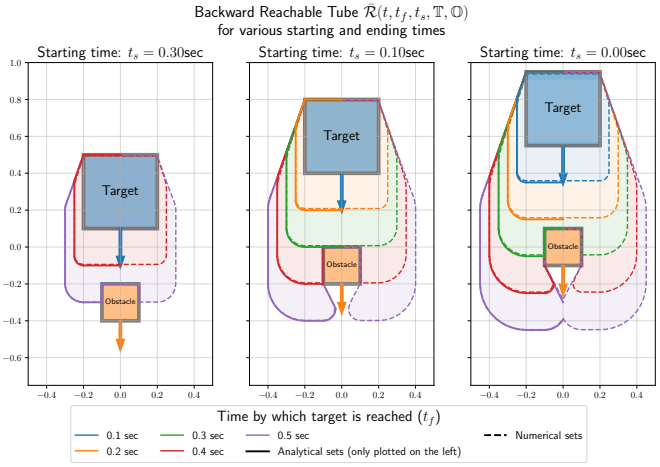

Fig. 1. Backward reachability tubes for various start and end times. Analytically computed tubes are superimposed in the left half on top of numerically computed tubes (dashed line).

B. Dynamic Dubin's car

1) Problem Setup: We now consider a more complex $3D$ dynamical system often referred to as the Dubin's car. The state space of the car is given by its position and orientation: $\boldsymbol{x} = [x, y, \theta]$. The only control is that of the steering rate $\dot{\theta} = u_\alpha$. The dynamics is given by

$$\begin{bmatrix}\dot{x} & \dot{y} & \dot{\theta}\end{bmatrix}^T = \begin{bmatrix}v\cos\theta & v\sin\theta & u_\alpha\end{bmatrix}^T,$$

where $v = 1$ is the velocity of the car. We additionally constrain the steering rate to satisfy $|u_\alpha| < \frac{\pi}{3}$ units.

We add a moving target and moving obstacle with velocities $[0.4, 0]$ and $[0.2, 0]$, respectively. The positions of the target and obstacle at various times are shown in Fig. 2 (the target is blue and obstacle orange). Our goal is to compute backward reachable tubes as well as time-to-reach maps.

2) Results: Since the state space is $3D$, the value function now lives in a $3D$ space. To get an intuition of what kind of information can be gained from the value function, we consider the duration map at a slice $\mathcal{D}(x, y, \theta = 8.95^o, t)$ (Fig. 2). At a given (x, y) and time t, the duration map returns the amount of time needed to reach the target when starting at that position and time, and being initially aligned at the given angle (i.e. $\theta = 8.95^o$). As expected, states to the left of the target can reach the target set more easily given their initial orientation (states to the right need to turn

around to reach the target set). In addition, note the triangular region which forms on the left of the obstacle, corresponding to regions where the car cannot avoid the obstacle.

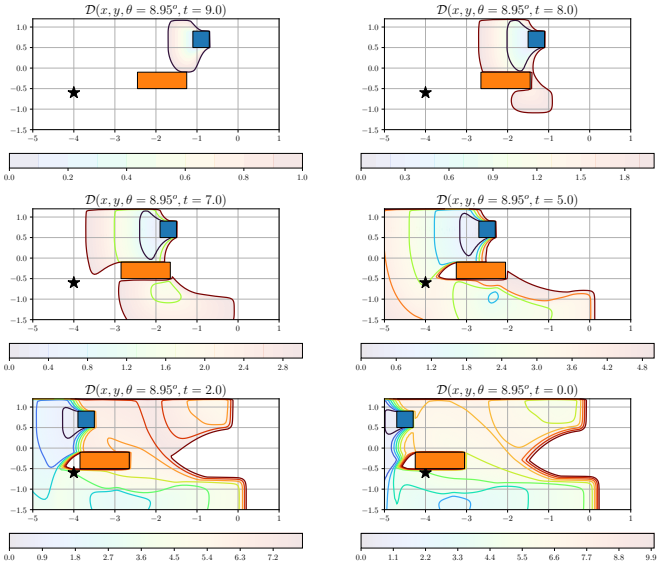

Fig. 2. Slice of the duration map at $\theta = 8.95^o$. This map physically represents the time needed to reach the target set based on the initial position of the car. The point marked with the star denotes an arbitrary start point that is used in subsequent analysis (Fig. 5).

Fig. 2 highlights a key feature of the power of multi-time reachability. Consider the following question: given a start point (x_s, y_s, θ_s) (marked with a star), what is the minimum duration to the target as a function of the start time (t_s)? This information is readily available using the duration map, $\mathcal{D}(x_s, y_s, \theta_s, t_s)$, as seen in Fig. 3. As different contours of the duration map reach the start point, we see vastly different gradients of the value function – implying changing optimal control strategies based on when the car starts.

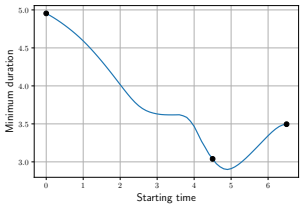

Fig. 3. Duration of the journey to the target set as a function of the starting time. Since this is a time varying system, the duration is not constant. Due to the moving obstacle, the duration first decreases and increases. Times of interest are marked with a black dot.

Suppose we pose another question: Given a start position (x_s, y_s) what is the optimal starting angle at different starting times to minimize the duration to the target set? We can use the following expression to compute the duration under optimal θ as a function of the starting time t_s: $d(t_s) = \min_\theta \mathcal{D}(x_s, y_s, \theta, t_s)$. The corresponding optimal θ is given by $\arg\min_\theta \mathcal{D}(x_s, y_s, \theta, t_s)$. Fig. 4 shows, for a start position $(x_s, y_s) = (-3, -0.7)$, this minimum duration and optimal θ as a function of start time. These plots, trivially generated using the multi-time reachability value function, contain information that is invaluable in deciding when and how to start the journey from a given start point.

Different regimes of the optimal solution can be noted, as

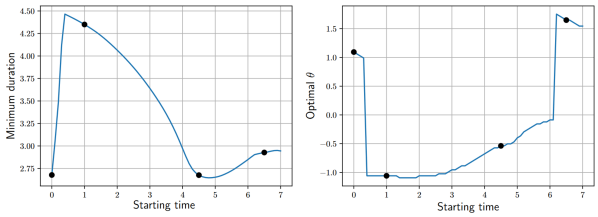

Fig. 4. (Left) Minimum duration to reach the target set, given the starting position $(x_s, y_s) = (-3, -0.7)$, as a function of starting time (t_s). (Right) Initial angle θ_s under which this minimum duration can be achieved for each corresponding starting time. Points of interest are marked with black dots.

the car decides to start with drastically different angles based on the starting time. To see why this is occurs, we plot the trajectories (Fig. 5) of all the points of interest marked with black dots in Figs. 3 and 4. The plot on the left traces out

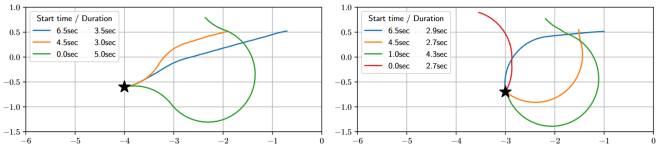

Fig. 5. Trajectories for various start points, start times and start angles. (Left) Trajectories starting at fixed start point but with the optimal angle to reach the destination as early as possible. (Right) Trajectories start at a constrained position and angle. Both set of trajectories start at a user defined time and end at different times before the final time horizon T

optimal trajectories when starting at the star (for various start times marked in Fig. 3) while constraining the initial heading the vehicle must start with. We find that the duration initially falls with start time as cutting across the front of the obstacle is difficult for the agent given this constrained initial angle. The plot on the right corresponds to the trajectories starting at optimal θ at various times (Fig. 4). We see that early on, the optimal agent cuts across the front of the obstacle and heads straight for the target. If it starts later, it has to go out of its way to drive around the front of the obstacle. However, if it waits long enough, the agent can reach the target by traversing behind the obstacle.

This case shows how we compute optimal trajectories for a variety of starting positions, angles, and start/terminal times. We further note that these can all be efficiently computed using information from a *single* multi-time reachability PDE solve – something not possible with other approaches.

C. AUV in a Bottom Gravity Current Flow Field

1) Problem Setup: Finally, we showcase results when a time-varying dynamic environment affects the system and optimal control. We consider an AUV in $2D$ with state variables $\boldsymbol{x} = (x, z)$ where x and z are position and depth of the vehicle. We denote the dynamics by

$$\dot{\boldsymbol{x}} = \begin{bmatrix} F_x \cos(u_\theta) + V_x(\boldsymbol{x}, t) & F_y \sin(u_\theta) + V_y(\boldsymbol{x}, t) \end{bmatrix}^T,$$

where u_θ is the sole control and $\boldsymbol{V} = [V_x, V_y]$ is the dynamic background ocean flow field that advects the AUV around. The background flow is that of a non-hydrostatic bottom gravity current simulated using our Finite Volume ocean modeling software [37]. This flow involves heavy salt water flowing down an incline and creating eddies due to Kevin-Helmholtz instabilities, as visualized in Fig. 6 [38].

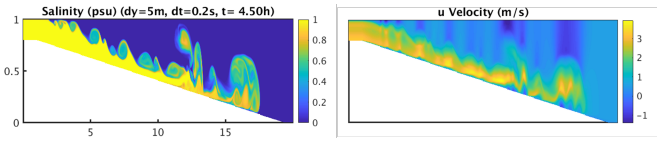

Fig. 6. Salinity field (left) and x-component of the velocity field in m/s (right) for the the bottom gravity flow. The units of x and y are in km.

2) Results: We consider a domain of interest at the bottom of the incline. As expected, we see that the duration map is uniform at the time before the current reaches the bottom, whereas it is non-uniform and time-varying at the time frame when the current and its billows and waves arrive (Fig. 7).

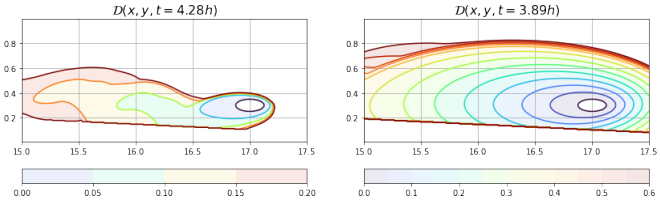

Fig. 7. Duration maps under the bottom gravity flow after (left) and before (right) the current enters the domain. The units of x and y are in km, and the unit for time is hours.

Applications of multi-time reachability to dynamic ocean environments can be found in [25].

VI. Conclusions

We obtained the governing equations for reachability over multiple start and terminal times all at once, for systems operating in time-varying environments with dynamic obstacles and any other relevant dynamic fields. We verified results analytically for a moving target and obstacle problem, then applied multi-time reachability to an extended dynamic Dubin's car, and finally showcased the method in a bottom gravity current system. Results highlight the novel capabilities of exact multi-time reachability in dynamic environments. Future work include stochastic effects, adaptive control, data assimilation, learning, and multi-time flow maps [39].

References

[1] S. Bansal, *et al.*, "Hamilton-jacobi reachability: A brief overview and recent advances," in *2017 IEEE 56th Annual Conference on Decision and Control (CDC)*. IEEE, 2017, pp. 2242–2253.

[2] M. Chen, *et al.*, "Decomposition of reachable sets and tubes for a class of nonlinear systems," *IEEE Transactions on Automatic Control*, vol. 63, no. 11, pp. 3675–3688, 2018.

[3] M. Chen and C. J. Tomlin, "Hamilton–jacobi reachability: Some recent theoretical advances and applications in unmanned airspace management," *Annual Review of Control, Robotics, and Autonomous Systems*, vol. 1, pp. 333–358, 2018.

[4] A. B. Kurzhanski and P. Varaiya, "Ellipsoidal techniques for reachability under state constraints," *SIAM Journal on Control and Optimization*, vol. 45, no. 4, pp. 1369–1394, 2006.

[5] O. Bokanowski, *et al.*, "Reachability and minimal times for state constrained nonlinear problems without any controllability assumption," *SIAM J. on Control and Optim.*, vol. 48, no. 7, pp. 4292–4316, 2010.

[6] O. Bokanowski and H. Zidani, "Minimal time problems with moving targets and obstacles," *IFAC Proceedings Volumes*, vol. 44, no. 1, pp. 2589–2593, 2011, 18th IFAC World Congress.

[7] J. F. Fisac, *et al.*, "Reach-avoid problems with time-varying dynamics, targets and constraints," in *Proc. of the 18th international conference on hybrid systems: computation and control*, 2015, pp. 11–20.

[8] T. Lolla, *et al.*, "Path planning in time dependent flow fields using level set methods," in *IEEE International Conference on Robotics and Automation (ICRA), 14-18 May 2012*, 2012, pp. 166–173.

[9] ——, "Time-optimal path planning in dynamic flows using level set equations: Theory and schemes," *Ocean Dynamics*, vol. 64, no. 10, pp. 1373–1397, 2014.

[10] ——, "Time-optimal path planning in dynamic flows using level set equations: Realistic applications," *Ocean Dynamics*, vol. 64, no. 10, pp. 1399–1417, 2014.

[11] G. Mannarini, *et al.*, "Graph-search and differential equations for time-optimal vessel route planning in dynamic ocean waves," *IEEE Trans. on Intelligent Transport. Systems*, vol. 21, no. 6, pp. 1–13, June 2020.

[12] D. N. Subramani, *et al.*, "Stochastic time-optimal path-planning in uncertain, strong, and dynamic flows," *Computer Methods in Applied Mechanics and Engineering*, vol. 333, pp. 218–237, 2018.

[13] D. N. Subramani and P. F. J. Lermusiaux, "Risk-optimal path planning in stochastic dynamic environments," *Computer Methods in Applied Mechanics and Engineering*, vol. 353, pp. 391–415, Aug. 2019.

[14] W. Sun, *et al.*, "Multiple-pursuer-one-evader pursuit evasion game in dynamic flow fields," *J. of Guid., Cont. and Dyn.*, vol. 40, no. 7, 2017.

[15] H. Huang, *et al.*, "A differential game approach to planning in adversarial scenarios: A case study on capture-the-flag," in *2011 IEEE Int. Conf. on Robotics and Automation*. IEEE, 2011, pp. 1451–1456.

[16] A. M. Bayen, *et al.*, "Aircraft autolander safety analysis through optimal control-based reach set computation," *Journal of Guidance, Control, and Dynamics*, vol. 30, no. 1, pp. 68–77, 2007.

[17] J. Ding, *et al.*, "Reachability calculations for automated aerial refueling," in *47th IEEE Conf. on Dec. & Con.* IEEE, 2008, pp. 3706–3712.

[18] A. Aswani, *et al.*, "Provably safe and robust learning-based model predictive control," *Automatica*, vol. 49, no. 5, pp. 1216–1226, 2013.

[19] P. F. J. Lermusiaux, *et al.*, "A future for intelligent autonomous ocean observing systems," *Journal of Marine Research*, vol. 75, no. 6, pp. 765–813, Nov. 2017.

[20] M. S. Bhabra, *et al.*, "Optimal harvesting with autonomous tow vessels for offshore macroalgae farming," in *OCEANS 2020 IEEE/MTS*. IEEE, Oct. 2020, pp. 1–10.

[21] A. B. Kurzhanski and P. Varaiya, "Dynamic optimization for reachability problems," *J. of Optimization Theory and Applications*, vol. 108, no. 2, pp. 227–251, 2001.

[22] L. Evans, *Partial Differential Equations*, ser. Graduate studies in mathematics. American Mathematical Society, 2010.

[23] D. Bertsekas, *Dynamic programming and optimal control: Volume I*. Athena scientific, 2012, vol. 1.

[24] D. E. Kirk, *Optimal control theory: an introduction*. Courier Corporation, 2004.

[25] M. Wiggert, *et al.*, "Navigating underactuated agents by hitchhiking forecast flows," in *2022 IEEE 61th Annual Conference on Decision and Control (CDC)*. IEEE, 2022.

[26] T. Lolla, *et al.*, "Path planning in multiscale ocean flows: Coordination and dynamic obstacles," *Ocean Modelling*, vol. 94, pp. 46–66, 2015.

[27] W. Liao and T. Liang, "Computation of reachable sets based on hamilton-jacobi-bellman equation with running cost function," 2021.

[28] S. Osher and R. P. Fedkiw, *Level set methods and dynamic implicit surfaces*. Springer New York, 2005, vol. 1.

[29] C.-W. Shu, "High order numerical methods for time dependent hamilton-jacobi equations," in *Mathematics and computation in imaging science and information processing*. World Sc., 2007, pp. 47–91.

[30] H. Lomax, *et al.*, *Fundamentals of computational fluid dynamics*. Springer Science & Business Media, 2013.

[31] J. S. Hesthaven and T. Warburton, *Nodal discontinuous Galerkin methods: algorithms, analysis, and applications*. Springer Science & Business Media, 2007.

[32] I. M. Mitchell *et al.*, "A toolbox of level set methods," *UBC Department of Computer Science Technical Report TR-2007-11*, p. 31, 2007.

[33] M. M. Doshi, *et al.*, "Energy-time optimal path planning in dynamic flows: Theory and schemes," 2022, sub-judice.

[34] M. S. Bhabra, *et al.*, "Harvest-time optimal path planning in dynamic flows," 2022, in preparation.

[35] E. Schmerling. (2022) hj_reachability - Online.

[36] J. Bradbury, *et al.*, "JAX: composable transformations of Python+NumPy programs," 2018.

[37] M. P. Ueckermann and P. F. J. Lermusiaux, "2.29 Finite Volume MATLAB Framework Documentation," Department of Mechanical Engineering, MIT, Cambridge, MA, MSEAS Report 14, 2012.

[38] J. Lin and P. F. J. Lermusiaux, "Bayesian learning of turbulent bottom gravity currents models," 2022, in preparation.

[39] C. S. Kulkarni and P. F. J. Lermusiaux, "Advection without compounding errors through flow map composition," *Journal of Computational Physics*, vol. 398, p. 108859, Dec. 2019.